

Measurement of the Ratio $\mathcal{B}(B^+ \rightarrow X e \nu)/\mathcal{B}(B^0 \rightarrow X e \nu)$

- B. Aubert,¹ M. Bona,¹ D. Boutigny,¹ F. Couderc,¹ Y. Karyotakis,¹ J. P. Lees,¹ V. Poireau,¹ V. Tisserand,¹ A. Zghiche,¹ E. Grauges,² A. Palano,³ J. C. Chen,⁴ N. D. Qi,⁴ G. Rong,⁴ P. Wang,⁴ Y. S. Zhu,⁴ G. Eigen,⁵ I. Ofte,⁵ B. Stugu,⁵ G. S. Abrams,⁶ M. Battaglia,⁶ D. N. Brown,⁶ J. Button-Shafer,⁶ R. N. Cahn,⁶ E. Charles,⁶ M. S. Gill,⁶ Y. Groysman,⁶ R. G. Jacobsen,⁶ J. A. Kadyk,⁶ L. T. Kerth,⁶ Yu. G. Kolomensky,⁶ G. Kukartsev,⁶ G. Lynch,⁶ L. M. Mir,⁶ T. J. Orimoto,⁶ M. Pripstein,⁶ N. A. Roe,⁶ M. T. Ronan,⁶ W. A. Wenzel,⁶ P. del Amo Sanchez,⁷ M. Barrett,⁷ K. E. Ford,⁷ A. J. Hart,⁷ T. J. Harrison,⁷ C. M. Hawkes,⁷ A. T. Watson,⁷ T. Held,⁸ H. Koch,⁸ B. Lewandowski,⁸ M. Pelizaeus,⁸ K. Peters,⁸ T. Schroeder,⁸ M. Steinke,⁸ J. T. Boyd,⁹ J. P. Burke,⁹ W. N. Cottingham,⁹ D. Walker,⁹ D. J. Asgeirsson,¹⁰ T. Cuhadar-Donszelmann,¹⁰ B. G. Fulsom,¹⁰ C. Hearty,¹⁰ N. S. Knecht,¹⁰ T. S. Mattison,¹⁰ J. A. McKenna,¹⁰ A. Khan,¹¹ P. Kyberd,¹¹ M. Saleem,¹¹ D. J. Sherwood,¹¹ L. Teodorescu,¹¹ V. E. Blinov,¹² A. D. Bukin,¹² V. P. Druzhinin,¹² V. B. Golubev,¹² A. P. Onuchin,¹² S. I. Serednyakov,¹² Yu. I. Skovpen,¹² E. P. Solodov,¹² K. Yu Todyshev,¹² M. Bondioli,¹³ M. Bruinsma,¹³ M. Chao,¹³ S. Curry,¹³ I. Eschrich,¹³ D. Kirkby,¹³ A. J. Lankford,¹³ P. Lund,¹³ M. Mandelkern,¹³ R. K. Mommesen,¹³ W. Roethel,¹³ D. P. Stoker,¹³ S. Abachi,¹⁴ C. Buchanan,¹⁴ S. D. Foulkes,¹⁵ J. W. Gary,¹⁵ O. Long,¹⁵ B. C. Shen,¹⁵ K. Wang,¹⁵ L. Zhang,¹⁵ H. K. Hadavand,¹⁶ E. J. Hill,¹⁶ H. P. Paar,¹⁶ S. Rahatlou,¹⁶ V. Sharma,¹⁶ J. W. Berryhill,¹⁷ C. Campagnari,¹⁷ A. Cunha,¹⁷ B. Dahmes,¹⁷ T. M. Hong,¹⁷ D. Kovalskyi,¹⁷ J. D. Richman,¹⁷ T. W. Beck,¹⁸ A. M. Eisner,¹⁸ C. J. Flacco,¹⁸ C. A. Heusch,¹⁸ J. Kroseberg,¹⁸ W. S. Lockman,¹⁸ G. Nesom,¹⁸ T. Schalk,¹⁸ B. A. Schumm,¹⁸ A. Seiden,¹⁸ P. Spradlin,¹⁸ D. C. Williams,¹⁸ M. G. Wilson,¹⁸ J. Albert,¹⁹ E. Chen,¹⁹ A. Dvoretskii,¹⁹ F. Fang,¹⁹ D. G. Hitlin,¹⁹ I. Narsky,¹⁹ T. Piatenko,¹⁹ F. C. Porter,¹⁹ A. Ryd,¹⁹ G. Mancinelli,²⁰ B. T. Meadows,²⁰ K. Mishra,²⁰ M. D. Sokoloff,²⁰ F. Blanc,²¹ P. C. Bloom,²¹ S. Chen,²¹ W. T. Ford,²¹ J. F. Hirschauer,²¹ A. Kreisel,²¹ M. Nagel,²¹ U. Nauenberg,²¹ A. Olivas,²¹ W. O. Ruddick,²¹ J. G. Smith,²¹ K. A. Ulmer,²¹ S. R. Wagner,²¹ J. Zhang,²¹ A. Chen,²² E. A. Eckhart,²² A. Soffer,²² W. H. Toki,²² R. J. Wilson,²² F. Winklmeier,²² Q. Zeng,²² D. D. Altenburg,²³ E. Feltresi,²³ A. Hauke,²³ H. Jasper,²³ J. Merkel,²³ A. Petzold,²³ B. Spaan,²³ T. Brandt,²⁴ V. Klose,²⁴ H. M. Lacker,²⁴ W. F. Mader,²⁴ R. Nogowski,²⁴ J. Schubert,²⁴ K. R. Schubert,²⁴ R. Schwierz,²⁴ J. E. Sundermann,²⁴ A. Volk,²⁴ D. Bernard,²⁵ G. R. Bonneau,²⁵ E. Latour,²⁵ Ch. Thiebaux,²⁵ M. Verderi,²⁵ P. J. Clark,²⁶ W. Graddl,²⁶ F. Muheim,²⁶ S. Playfer,²⁶ A. I. Robertson,²⁶ Y. Xie,²⁶ M. Andreotti,²⁷ D. Bettoni,²⁷ C. Bozzi,²⁷ R. Calabrese,²⁷ G. Cibinetto,²⁷ E. Luppi,²⁷ M. Negrini,²⁷ A. Petrella,²⁷ L. Piemontese,²⁷ E. Prencipe,²⁷ F. Anulli,²⁸ R. Baldini-Ferroli,²⁸ A. Calcaterra,²⁸ R. de Sangro,²⁸ G. Finocchiaro,²⁸ S. Pacetti,²⁸ P. Patteri,²⁸ I. M. Peruzzi,²⁸, * M. Piccolo,²⁸ M. Rama,²⁸ A. Zallo,²⁸ A. Buzzo,²⁹ R. Contri,²⁹ M. Lo Vetere,²⁹ M. M. Macri,²⁹ M. R. Monge,²⁹ S. Passaggio,²⁹ C. Patrignani,²⁹ E. Robutti,²⁹ A. Santroni,²⁹ S. Tosi,²⁹ G. Brandenburg,³⁰ K. S. Chaisanguanthum,³⁰ M. Morii,³⁰ J. Wu,³⁰ R. S. Dubitzky,³¹ J. Marks,³¹ S. Schenck,³¹ U. Uwer,³¹ W. Bhimji,³² D. A. Bowerman,³² P. D. Dauncey,³² U. Egede,³² R. L. Flack,³² J. A. Nash,³² M. B. Nikolich,³² W. Panduro Vazquez,³² D. J. Bard,³³ P. K. Behera,³³ X. Chai,³³ M. J. Charles,³³ U. Mallik,³³ N. T. Meyer,³³ V. Ziegler,³³ J. Cochran,³⁴ H. B. Crawley,³⁴ L. Dong,³⁴ V. Eyges,³⁴ W. T. Meyer,³⁴ S. Prell,³⁴ E. I. Rosenberg,³⁴ A. E. Rubin,³⁴ A. V. Gritsan,³⁵ A. G. Denig,³⁶ M. Fritsch,³⁶ G. Schott,³⁶ N. Arnaud,³⁷ M. Davier,³⁷ G. Grosdidier,³⁷ A. Höcker,³⁷ F. Le Diberder,³⁷ V. Lepeltier,³⁷ A. M. Lutz,³⁷ A. Oyanguren,³⁷ S. Pruvot,³⁷ S. Rodier,³⁷ P. Roudeau,³⁷ M. H. Schune,³⁷ A. Stocchi,³⁷ W. F. Wang,³⁷ G. Wormser,³⁷ C. H. Cheng,³⁸ D. J. Lange,³⁸ D. M. Wright,³⁸ C. A. Chavez,³⁹ I. J. Forster,³⁹ J. R. Fry,³⁹ E. Gabathuler,³⁹ R. Gamet,³⁹ K. A. George,³⁹ D. E. Hutchcroft,³⁹ D. J. Payne,³⁹ K. C. Schofield,³⁹ C. Touramanis,³⁹ A. J. Bevan,⁴⁰ F. Di Lodovico,⁴⁰ W. Menges,⁴⁰ R. Sacco,⁴⁰ G. Cowan,⁴¹ H. U. Flaecher,⁴¹ D. A. Hopkins,⁴¹ P. S. Jackson,⁴¹ T. R. McMahon,⁴¹ S. Ricciardi,⁴¹ F. Salvatore,⁴¹ A. C. Wren,⁴¹ D. N. Brown,⁴² C. L. Davis,⁴² J. Allison,⁴³ N. R. Barlow,⁴³ R. J. Barlow,⁴³ Y. M. Chia,⁴³ C. L. Edgar,⁴³ G. D. Lafferty,⁴³ M. T. Naisbit,⁴³ J. C. Williams,⁴³ J. I. Yi,⁴³ C. Chen,⁴⁴ W. D. Hulsbergen,⁴⁴ A. Jawahery,⁴⁴ C. K. Lae,⁴⁴ D. A. Roberts,⁴⁴ G. Simi,⁴⁴ G. Blaylock,⁴⁵ C. Dallapiccola,⁴⁵ S. S. Hertzbach,⁴⁵ X. Li,⁴⁵ T. B. Moore,⁴⁵ S. Saremi,⁴⁵ H. Staengle,⁴⁵ R. Cowan,⁴⁶ G. Sciolla,⁴⁶ S. J. Sekula,⁴⁶ M. Spitznagel,⁴⁶ F. Taylor,⁴⁶ R. K. Yamamoto,⁴⁶ H. Kim,⁴⁷ S. E. McLachlin,⁴⁷ P. M. Patel,⁴⁷ S. H. Robertson,⁴⁷ A. Lazzaro,⁴⁸ V. Lombardo,⁴⁸ F. Palombo,⁴⁸ J. M. Bauer,⁴⁹ L. Cremaldi,⁴⁹ V. Eschenburg,⁴⁹

R. Godang,⁴⁹ R. Kroeger,⁴⁹ D. A. Sanders,⁴⁹ D. J. Summers,⁴⁹ H. W. Zhao,⁴⁹ S. Brunet,⁵⁰ D. Côté,⁵⁰ M. Simard,⁵⁰ P. Taras,⁵⁰ F. B. Viaud,⁵⁰ H. Nicholson,⁵¹ N. Cavallo,^{52,†} G. De Nardo,⁵² F. Fabozzi,^{52,†} C. Gatto,⁵² L. Lista,⁵² D. Monorchio,⁵² P. Paolucci,⁵² D. Piccolo,⁵² C. Sciacca,⁵² M. A. Baak,⁵³ G. Raven,⁵³ H. L. Snoek,⁵³ C. P. Jessop,⁵⁴ J. M. LoSecco,⁵⁴ T. Allmendinger,⁵⁵ G. Benelli,⁵⁵ L. A. Corwin,⁵⁵ K. K. Gan,⁵⁵ K. Honscheid,⁵⁵ D. Hufnagel,⁵⁵ P. D. Jackson,⁵⁵ H. Kagan,⁵⁵ R. Kass,⁵⁵ A. M. Rahimi,⁵⁵ J. J. Regensburger,⁵⁵ R. Ter-Antonyan,⁵⁵ Q. K. Wong,⁵⁵ N. L. Blount,⁵⁶ J. Brau,⁵⁶ R. Frey,⁵⁶ O. Igonkina,⁵⁶ J. A. Kolb,⁵⁶ M. Lu,⁵⁶ R. Rahmat,⁵⁶ N. B. Sinev,⁵⁶ D. Strom,⁵⁶ J. Strube,⁵⁶ E. Torrence,⁵⁶ A. Gaz,⁵⁷ M. Margoni,⁵⁷ M. Morandin,⁵⁷ A. Pompili,⁵⁷ M. Posocco,⁵⁷ M. Rotondo,⁵⁷ F. Simonetto,⁵⁷ R. Stroili,⁵⁷ C. Voci,⁵⁷ M. Benayoun,⁵⁸ H. Briand,⁵⁸ J. Chauveau,⁵⁸ P. David,⁵⁸ L. Del Buono,⁵⁸ Ch. de la Vaissière,⁵⁸ O. Hamon,⁵⁸ B. L. Hartfiel,⁵⁸ Ph. Leruste,⁵⁸ J. Malclès,⁵⁸ J. Ocariz,⁵⁸ L. Roos,⁵⁸ G. Therin,⁵⁸ L. Gladney,⁵⁹ M. Biasini,⁶⁰ R. Covarelli,⁶⁰ C. Angelini,⁶¹ G. Batignani,⁶¹ S. Bettarini,⁶¹ F. Bucci,⁶¹ G. Calderini,⁶¹ M. Carpinelli,⁶¹ R. Cenci,⁶¹ F. Forti,⁶¹ M. A. Giorgi,⁶¹ A. Lusiani,⁶¹ G. Marchiori,⁶¹ M. A. Mazur,⁶¹ M. Morganti,⁶¹ N. Neri,⁶¹ E. Paoloni,⁶¹ G. Rizzo,⁶¹ J. J. Walsh,⁶¹ M. Haire,⁶² D. Judd,⁶² D. E. Wagoner,⁶² J. Biesiada,⁶³ N. Danielson,⁶³ P. Elmer,⁶³ Y. P. Lau,⁶³ C. Lu,⁶³ J. Olsen,⁶³ A. J. S. Smith,⁶³ A. V. Telnov,⁶³ F. Bellini,⁶⁴ G. Cavoto,⁶⁴ A. D'Orazio,⁶⁴ D. del Re,⁶⁴ E. Di Marco,⁶⁴ R. Faccini,⁶⁴ F. Ferrarotto,⁶⁴ F. Ferroni,⁶⁴ M. Gaspero,⁶⁴ L. Li Gioi,⁶⁴ M. A. Mazzoni,⁶⁴ S. Morganti,⁶⁴ G. Piredda,⁶⁴ F. Polci,⁶⁴ F. Safai Tehrani,⁶⁴ C. Voena,⁶⁴ M. Ebert,⁶⁵ H. Schröder,⁶⁵ R. Waldi,⁶⁵ T. Adye,⁶⁶ N. De Groot,⁶⁶ B. Franek,⁶⁶ E. O. Olaiya,⁶⁶ F. F. Wilson,⁶⁶ R. Aleksan,⁶⁷ S. Emery,⁶⁷ A. Gaidot,⁶⁷ S. F. Ganzhur,⁶⁷ G. Hamel de Monchenault,⁶⁷ W. Kozanecki,⁶⁷ M. Legendre,⁶⁷ G. Vasseur,⁶⁷ Ch. Yèche,⁶⁷ M. Zito,⁶⁷ X. R. Chen,⁶⁸ H. Liu,⁶⁸ W. Park,⁶⁸ M. V. Purohit,⁶⁸ J. R. Wilson,⁶⁸ M. T. Allen,⁶⁹ D. Aston,⁶⁹ R. Bartoldus,⁶⁹ P. Bechtle,⁶⁹ N. Berger,⁶⁹ R. Claus,⁶⁹ J. P. Coleman,⁶⁹ M. R. Convery,⁶⁹ M. Cristinziani,⁶⁹ J. C. Dingfelder,⁶⁹ J. Dorfan,⁶⁹ G. P. Dubois-Felsmann,⁶⁹ D. Dujmic,⁶⁹ W. Dunwoodie,⁶⁹ R. C. Field,⁶⁹ T. Glanzman,⁶⁹ S. J. Gowdy,⁶⁹ M. T. Graham,⁶⁹ P. Grenier,⁶⁹ V. Halyo,⁶⁹ C. Hast,⁶⁹ T. Hrynn'ova,⁶⁹ W. R. Innes,⁶⁹ M. H. Kelsey,⁶⁹ P. Kim,⁶⁹ D. W. G. S. Leith,⁶⁹ S. Li,⁶⁹ S. Luitz,⁶⁹ V. Luth,⁶⁹ H. L. Lynch,⁶⁹ D. B. MacFarlane,⁶⁹ H. Marsiske,⁶⁹ R. Messner,⁶⁹ D. R. Muller,⁶⁹ C. P. O'Grady,⁶⁹ V. E. Ozcan,⁶⁹ A. Perazzo,⁶⁹ M. Perl,⁶⁹ T. Pulliam,⁶⁹ B. N. Ratcliff,⁶⁹ A. Roodman,⁶⁹ A. A. Salnikov,⁶⁹ R. H. Schindler,⁶⁹ J. Schwiening,⁶⁹ A. Snyder,⁶⁹ J. Stelzer,⁶⁹ D. Su,⁶⁹ M. K. Sullivan,⁶⁹ K. Suzuki,⁶⁹ S. K. Swain,⁶⁹ J. M. Thompson,⁶⁹ J. Va'vra,⁶⁹ N. van Bakel,⁶⁹ M. Weaver,⁶⁹ A. J. R. Weinstein,⁶⁹ W. J. Wisniewski,⁶⁹ M. Wittgen,⁶⁹ D. H. Wright,⁶⁹ A. K. Yarritu,⁶⁹ K. Yi,⁶⁹ C. C. Young,⁶⁹ P. R. Burchat,⁷⁰ A. J. Edwards,⁷⁰ S. A. Majewski,⁷⁰ B. A. Petersen,⁷⁰ C. Roat,⁷⁰ L. Wilden,⁷⁰ S. Ahmed,⁷¹ M. S. Alam,⁷¹ R. Bula,⁷¹ J. A. Ernst,⁷¹ V. Jain,⁷¹ B. Pan,⁷¹ M. A. Saeed,⁷¹ F. R. Wappeler,⁷¹ S. B. Zain,⁷¹ W. Bugg,⁷² M. Krishnamurthy,⁷² S. M. Spanier,⁷² R. Eckmann,⁷³ J. L. Ritchie,⁷³ A. Satpathy,⁷³ C. J. Schilling,⁷³ R. F. Schwitters,⁷³ J. M. Izen,⁷⁴ X. C. Lou,⁷⁴ S. Ye,⁷⁴ F. Bianchi,⁷⁵ F. Gallo,⁷⁵ D. Gamba,⁷⁵ M. Bomben,⁷⁶ L. Bosisio,⁷⁶ C. Cartaro,⁷⁶ F. Cossutti,⁷⁶ G. Della Ricca,⁷⁶ S. Dittongo,⁷⁶ L. Lanceri,⁷⁶ L. Vitale,⁷⁶ V. Azzolini,⁷⁷ N. Lopez-March,⁷⁷ F. Martinez-Vidal,⁷⁷ Sw. Banerjee,⁷⁸ B. Bhuyan,⁷⁸ C. M. Brown,⁷⁸ D. Fortin,⁷⁸ K. Hamano,⁷⁸ R. Kowalewski,⁷⁸ I. M. Nugent,⁷⁸ J. M. Roney,⁷⁸ R. J. Sobie,⁷⁸ J. J. Back,⁷⁹ P. F. Harrison,⁷⁹ T. E. Latham,⁷⁹ G. B. Mohanty,⁷⁹ M. Pappagallo,⁷⁹ H. R. Band,⁸⁰ X. Chen,⁸⁰ B. Cheng,⁸⁰ S. Dasu,⁸⁰ M. Datta,⁸⁰ K. T. Flood,⁸⁰ J. J. Hollar,⁸⁰ P. E. Kutter,⁸⁰ B. Mellado,⁸⁰ A. Mihalyi,⁸⁰ Y. Pan,⁸⁰ M. Pierini,⁸⁰ R. Prepost,⁸⁰ S. L. Wu,⁸⁰ Z. Yu,⁸⁰ and H. Neal⁸¹

(The BABAR Collaboration)

¹Laboratoire de Physique des Particules, IN2P3/CNRS et Université de Savoie, F-74941 Annecy-Le-Vieux, France

²Universitat de Barcelona, Facultat de Fisica, Departament ECM, E-08028 Barcelona, Spain

³Università di Bari, Dipartimento di Fisica and INFN, I-70126 Bari, Italy

⁴Institute of High Energy Physics, Beijing 100039, China

⁵University of Bergen, Institute of Physics, N-5007 Bergen, Norway

⁶Lawrence Berkeley National Laboratory and University of California, Berkeley, California 94720, USA

⁷University of Birmingham, Birmingham, B15 2TT, United Kingdom

⁸Ruhr Universität Bochum, Institut für Experimentalphysik 1, D-44780 Bochum, Germany

⁹University of Bristol, Bristol BS8 1TL, United Kingdom

¹⁰University of British Columbia, Vancouver, British Columbia, Canada V6T 1Z1

¹¹Brunel University, Uxbridge, Middlesex UB8 3PH, United Kingdom

¹²Budker Institute of Nuclear Physics, Novosibirsk 630090, Russia

¹³University of California at Irvine, Irvine, California 92697, USA

¹⁴University of California at Los Angeles, Los Angeles, California 90024, USA

¹⁵University of California at Riverside, Riverside, California 92521, USA

- ¹⁶*University of California at San Diego, La Jolla, California 92093, USA*
- ¹⁷*University of California at Santa Barbara, Santa Barbara, California 93106, USA*
- ¹⁸*University of California at Santa Cruz, Institute for Particle Physics, Santa Cruz, California 95064, USA*
- ¹⁹*California Institute of Technology, Pasadena, California 91125, USA*
- ²⁰*University of Cincinnati, Cincinnati, Ohio 45221, USA*
- ²¹*University of Colorado, Boulder, Colorado 80309, USA*
- ²²*Colorado State University, Fort Collins, Colorado 80523, USA*
- ²³*Universität Dortmund, Institut für Physik, D-44221 Dortmund, Germany*
- ²⁴*Technische Universität Dresden, Institut für Kern- und Teilchenphysik, D-01062 Dresden, Germany*
- ²⁵*Laboratoire Leprince-Ringuet, CNRS/IN2P3, Ecole Polytechnique, F-91128 Palaiseau, France*
- ²⁶*University of Edinburgh, Edinburgh EH9 3JZ, United Kingdom*
- ²⁷*Università di Ferrara, Dipartimento di Fisica and INFN, I-44100 Ferrara, Italy*
- ²⁸*Laboratori Nazionali di Frascati dell'INFN, I-00044 Frascati, Italy*
- ²⁹*Università di Genova, Dipartimento di Fisica and INFN, I-16146 Genova, Italy*
- ³⁰*Harvard University, Cambridge, Massachusetts 02138, USA*
- ³¹*Universität Heidelberg, Physikalisches Institut, Philosophenweg 12, D-69120 Heidelberg, Germany*
- ³²*Imperial College London, London, SW7 2AZ, United Kingdom*
- ³³*University of Iowa, Iowa City, Iowa 52242, USA*
- ³⁴*Iowa State University, Ames, Iowa 50011-3160, USA*
- ³⁵*Johns Hopkins University, Baltimore, Maryland 21218, USA*
- ³⁶*Universität Karlsruhe, Institut für Experimentelle Kernphysik, D-76021 Karlsruhe, Germany*
- ³⁷*Laboratoire de l'Accélérateur Linéaire, IN2P3/CNRS et Université Paris-Sud 11, Centre Scientifique d'Orsay, B.P. 34, F-91898 ORSAY Cedex, France*
- ³⁸*Lawrence Livermore National Laboratory, Livermore, California 94550, USA*
- ³⁹*University of Liverpool, Liverpool L69 7ZE, United Kingdom*
- ⁴⁰*Queen Mary, University of London, E1 4NS, United Kingdom*
- ⁴¹*University of London, Royal Holloway and Bedford New College, Egham, Surrey TW20 0EX, United Kingdom*
- ⁴²*University of Louisville, Louisville, Kentucky 40292, USA*
- ⁴³*University of Manchester, Manchester M13 9PL, United Kingdom*
- ⁴⁴*University of Maryland, College Park, Maryland 20742, USA*
- ⁴⁵*University of Massachusetts, Amherst, Massachusetts 01003, USA*
- ⁴⁶*Massachusetts Institute of Technology, Laboratory for Nuclear Science, Cambridge, Massachusetts 02139, USA*
- ⁴⁷*McGill University, Montréal, Québec, Canada H3A 2T8*
- ⁴⁸*Università di Milano, Dipartimento di Fisica and INFN, I-20133 Milano, Italy*
- ⁴⁹*University of Mississippi, University, Mississippi 38677, USA*
- ⁵⁰*Université de Montréal, Physique des Particules, Montréal, Québec, Canada H3C 3J7*
- ⁵¹*Mount Holyoke College, South Hadley, Massachusetts 01075, USA*
- ⁵²*Università di Napoli Federico II, Dipartimento di Scienze Fisiche and INFN, I-80126, Napoli, Italy*
- ⁵³*NIKHEF, National Institute for Nuclear Physics and High Energy Physics, NL-1009 DB Amsterdam, The Netherlands*
- ⁵⁴*University of Notre Dame, Notre Dame, Indiana 46556, USA*
- ⁵⁵*Ohio State University, Columbus, Ohio 43210, USA*
- ⁵⁶*University of Oregon, Eugene, Oregon 97403, USA*
- ⁵⁷*Università di Padova, Dipartimento di Fisica and INFN, I-35131 Padova, Italy*
- ⁵⁸*Laboratoire de Physique Nucléaire et de Hautes Energies, IN2P3/CNRS, Université Pierre et Marie Curie-Paris6, Université Denis Diderot-Paris7, F-75252 Paris, France*
- ⁵⁹*University of Pennsylvania, Philadelphia, Pennsylvania 19104, USA*
- ⁶⁰*Università di Perugia, Dipartimento di Fisica and INFN, I-06100 Perugia, Italy*
- ⁶¹*Università di Pisa, Dipartimento di Fisica, Scuola Normale Superiore and INFN, I-56127 Pisa, Italy*
- ⁶²*Prairie View A&M University, Prairie View, Texas 77446, USA*
- ⁶³*Princeton University, Princeton, New Jersey 08544, USA*
- ⁶⁴*Università di Roma La Sapienza, Dipartimento di Fisica and INFN, I-00185 Roma, Italy*
- ⁶⁵*Universität Rostock, D-18051 Rostock, Germany*
- ⁶⁶*Rutherford Appleton Laboratory, Chilton, Didcot, Oxon, OX11 0QX, United Kingdom*
- ⁶⁷*DSM/Dapnia, CEA/Saclay, F-91191 Gif-sur-Yvette, France*
- ⁶⁸*University of South Carolina, Columbia, South Carolina 29208, USA*
- ⁶⁹*Stanford Linear Accelerator Center, Stanford, California 94309, USA*
- ⁷⁰*Stanford University, Stanford, California 94305-4060, USA*
- ⁷¹*State University of New York, Albany, New York 12222, USA*
- ⁷²*University of Tennessee, Knoxville, Tennessee 37996, USA*
- ⁷³*University of Texas at Austin, Austin, Texas 78712, USA*

⁷⁴*University of Texas at Dallas, Richardson, Texas 75083, USA*

⁷⁵*Università di Torino, Dipartimento di Fisica Sperimentale and INFN, I-10125 Torino, Italy*

⁷⁶*Università di Trieste, Dipartimento di Fisica and INFN, I-34127 Trieste, Italy*

⁷⁷*IFIC, Universitat de Valencia-CSIC, E-46071 Valencia, Spain*

⁷⁸*University of Victoria, Victoria, British Columbia, Canada V8W 3P6*

⁷⁹*Department of Physics, University of Warwick, Coventry CV4 7AL, United Kingdom*

⁸⁰*University of Wisconsin, Madison, Wisconsin 53706, USA*

⁸¹*Yale University, New Haven, Connecticut 06511, USA*

We report measurements of the inclusive electron momentum spectra in decays of charged and neutral B mesons, and of the ratio of semileptonic branching fractions $\mathcal{B}(B^+ \rightarrow Xe\nu)$ and $\mathcal{B}(B^0 \rightarrow Xe\nu)$. These were performed on a sample of 231 million $B\bar{B}$ events recorded with the *BABAR* detector at the $\Upsilon(4S)$ resonance. Events are selected by fully reconstructing a hadronic decay of one B meson and identifying an electron among the decay products of the recoiling \bar{B} meson. We obtain $\mathcal{B}(B^+ \rightarrow Xe\nu)/\mathcal{B}(B^0 \rightarrow Xe\nu) = 1.084 \pm 0.041_{\text{(stat)}} \pm 0.025_{\text{(syst)}}$.

PACS numbers: 12.15.Hh, 11.30.Er, 13.25.Hw

The hadronic decay widths of B^+ and B^0 mesons differ because of mechanisms that depend on the flavor of the spectator quark, such as interactions involving the spectator quark or final state particles. This leads to different lifetimes τ_{B^+} and τ_{B^0} of charged and neutral B mesons. We do not expect different semileptonic decay widths, since semileptonic decays do not involve the spectator quark. This means that the ratio $R_{+/0} = \mathcal{B}(B^+ \rightarrow Xe\nu)/\mathcal{B}(B^0 \rightarrow Xe\nu)$ should agree with τ_{B^+}/τ_{B^0} , which can be checked experimentally.

At the $\Upsilon(4S)$ resonance, measurements of the inclusive semileptonic branching fractions of B^+ and B^0 mesons are less precise than for an admixture of b hadrons. The reason is mainly a limitation of statistics from the small efficiency of the event tag needed to separate B^+B^- from $B^0\bar{B}^0$ events. In this paper, we use fully reconstructed hadronic B decays for this separation. Combined with the high statistics of the B factories, this approach allows for a precision measurement of $R_{+/0}$, as already demonstrated by the Belle collaboration, measuring $R_{+/0}$ with 5% uncertainty [1]. By tagging $B^0\bar{B}^0$ events with partially reconstructed $B^0 \rightarrow D^{*-}\ell\nu$ decays, the CLEO collaboration achieved a 14% uncertainty on $R_{+/0}$ [2]. High-momentum electron tags have been used in similar analyses for the determination of $\mathcal{B}(B \rightarrow Xe\nu)$ and the electron momentum spectrum without separation of B^0 and B^+ decays [3, 4].

The measurements presented here are based on data collected by the *BABAR* detector [5] at the PEP-II asymmetric e^+e^- storage rings and correspond to an integrated luminosity of 209 fb^{-1} (231 million $B\bar{B}$ events) on the $\Upsilon(4S)$ resonance. For background and efficiency corrections that cannot be measured directly from data, we use a full simulation of the detector based on GEANT4 [6]. The equivalent luminosity of the simulated event sample amounts to about 980 fb^{-1} for $\Upsilon(4S) \rightarrow B\bar{B}$ events and 300 fb^{-1} for processes consisting of non-resonant $e^+e^- \rightarrow q\bar{q}$ ($q = u, d, s, c$) production

(“continuum events”).

In events with a fully reconstructed hadronic B decay (B_{tag}), we identify electrons among the remaining tracks. To avoid large backgrounds at lower momenta, we require $p_e > 0.6 \text{ GeV}/c$, where p_e is the electron momentum measured in the center-of-mass frame. Depending on the electron charge q_e relative to the charge q_b of the bottom quark in the B_{tag} candidate, each electron is assigned to either the right-sign ($q_e = -3q_b$) or to the wrong-sign sample ($q_e = 3q_b$). In events without $B^0\bar{B}^0$ -mixing and a correctly reconstructed B_{tag} , primary electrons from semileptonic decays of the signal B are the dominant source for the right-sign sample, while electrons from $B \rightarrow \bar{D}X, \bar{D} \rightarrow e^-\nu_e Y$ cascades populate the wrong-sign sample. We use the criteria in Ref. [3] for track selection and electron identification, and apply the same procedures for efficiency and background corrections of the right- and wrong-sign samples. In this analysis, we additionally have to correct for mis-reconstructed B_{tag} candidates.

Non- $B\bar{B}$ events are suppressed by requiring the ratio of the second to the zeroth Fox-Wolfram moments [7] to be less than 0.5. To keep backgrounds from mis-reconstructed B_{tag} candidates at a low level, we reconstruct hadronic B decays in very pure modes only. To cancel systematic errors related to the B_{tag} reconstruction, we select similar (“twin”) modes for B^0 and B^+ decays [8]:

(I) $B^0 \rightarrow \pi(K\pi\pi)_{D^-}$	$B^+ \rightarrow \pi(K\pi\pi^0)_{\bar{D}^0}$
(II) $B^0 \rightarrow \pi[(K\pi)_{\bar{D}^0}\pi]_{D^{*-}}$	$B^+ \rightarrow \pi[(K\pi)_{\bar{D}^0}\pi^0]_{\bar{D}^{*0}}$
(III) $B^0 \rightarrow \pi\pi\pi[(K\pi)_{\bar{D}^0}\pi]_{D^{*-}}$	$B^+ \rightarrow \pi\pi\pi[(K\pi)_{\bar{D}^0}\pi^0]_{\bar{D}^{*0}}$
(IV) $B^0 \rightarrow \pi[(K\pi\pi^0)_{\bar{D}^0}\pi]_{D^{*-}}$	$B^+ \rightarrow \pi[(K\pi\pi^0)_{\bar{D}^0}\pi^0]_{\bar{D}^{*0}}$
(V) $B^0 \rightarrow \pi\pi^0[(K\pi)_{\bar{D}^0}\pi]_{D^{*-}}$	$B^+ \rightarrow \pi\pi^0[(K\pi)_{\bar{D}^0}\pi^0]_{\bar{D}^{*0}}$

Here π and K denote charged pions and kaons. The invariant mass of \bar{D}^0 candidates is required to be within $15 \text{ MeV}/c^2$ of the nominal \bar{D}^0 mass [9] for the decay

$\bar{D}^0 \rightarrow K\pi$ and 25 MeV/ c^2 for $\bar{D}^0 \rightarrow K\pi\pi^0$ decays. D^- candidates are accepted if the invariant mass is within 20 MeV/ c^2 of the nominal D^- mass. D candidates with momenta above 2.5 GeV/ c (measured in the center-of-mass frame) are rejected since they indicate non- $B\bar{B}$ events. D^* candidates are built from pairs of \bar{D}^0 candidates and charged (neutral) pions where the invariant mass difference $|M_{\bar{D}^0\pi^{(0)}} - M_{\bar{D}^0}|$ is within 2 MeV/ c^2 of the nominal mass difference. In tag categories (III) and (V) we require the invariant masses $M_{\pi\pi\pi}$ and $M_{\pi\pi^0}$ to be less than 1.5 GeV/ c^2 . For further background reduction, we reject candidates where a kinematic fit with geometric constraints on the B and D vertices and mass constraints on the charmed mesons yields a χ^2 value with a probability of less than 0.5%.

The kinematic consistency of the B_{tag} candidates is checked with two variables, the beam-energy substituted mass $m_{ES} = (s/4 - p_B^2)^{1/2}$ and the energy difference $\Delta E = E_B - \sqrt{s}/2$. Here \sqrt{s} refers to the total center-of-mass energy, and E_B and p_B denote the energy and momentum of the B_{tag} candidate, all quantities being measured in the center-of-mass frame. For categories (I) - (III), we require $|\Delta E| < 50$ MeV, while the presence of an additional π^0 in (IV) and (V) leads to asymmetric distributions in ΔE , motivating lower limits of $\Delta E > -75$ MeV for (IV) and $\Delta E > -100$ MeV for (V). If for a given mode more than one B_{tag} candidate satisfies these criteria, the one with the smallest $|\Delta E|$ is selected. Figure 1 shows the m_{ES} distributions of B_{tag} candidates satisfying these selection criteria. Candidates with $5.27 < m_{ES} < 5.29$ GeV/ c^2 are included in the B_{tag} sample. In $\approx 1\%$ of all events, we find multiple B_{tag} candidates in different decay modes. Here we use all of them, correcting for the background B_{tag} candidates later.

The B_{tag} sample can be divided into 4 components: signal, combinatoric background, $D^{*-} \leftrightarrow \bar{D}^{*0}$ cross feed and continuum background. Correctly reconstructed B decays are called *signal* B_{tag} candidates, while B_{tag} candidates that contain tracks from the decay of the other B contribute to the *combinatoric* B_{tag} background. A special case of combinatoric background, called $D^{*-} \leftrightarrow \bar{D}^{*0}$ cross feed, contains cross feeds between twin modes of channels (II)-(V) due to mis-reconstruction of a D^{*-} as a \bar{D}^{*0} or vice versa. Due to the low energy of the combinatoric pion, the m_{ES} distribution of this background is similar to the signal and will be treated separately from the other combinatoric B_{tag} background. The fourth component consists of B_{tag} candidates arising from continuum events and is called *continuum* B_{tag} background. Since the ratio of signal to background B_{tag} candidates depends on the multiplicity of the event and thus on the presence of a semileptonic decay, a precise determination of the number of signal B_{tag} candidates is crucial to avoid biases in the branching fraction measurement.

Monte Carlo (MC) studies using generator information indicate that once the B_{tag} , right- and wrong-sign samples have been corrected for B_{tag} background, the biases on the branching fraction measurements are below the statistical sensitivity given by the size of the MC sample, i.e. less than 0.5%.

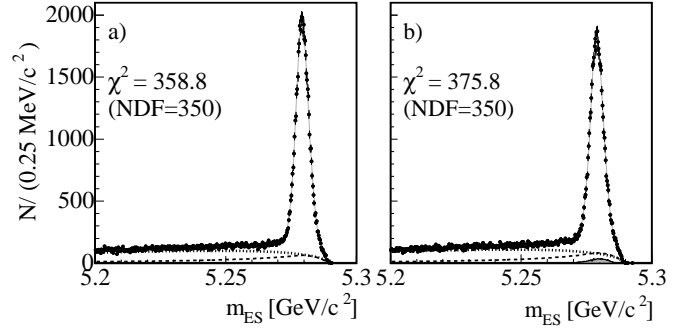


FIG. 1: Fits of Eq. 1 to distributions of the energy substituted mass for (a) neutral and (b) charged B_{tag} candidates. The dotted and dashed curves indicate the fitted contributions of continuum and combinatoric B_{tag} candidates. The grey histogram displays the contribution of $D^{*-} \leftrightarrow \bar{D}^{*0}$ background.

The contributions of combinatoric and continuum B_{tag} background to the B_{tag} sample are extrapolated from the m_{ES} sideband region, $5.2 < m_{ES} < 5.25$ GeV/ c^2 . This requires a model of the background m_{ES} distributions over the full range, $5.2 < m_{ES} < 5.29$ GeV/ c^2 , which is obtained by fitting a linear combination of three functions describing the shapes of m_{ES} distributions of signal, combinatoric and continuum B_{tag} candidates to the observed m_{ES} distributions.

The shape of the combinatoric B_{tag} background $f_{b\bar{b}}(m_{ES})$ is taken from the MC simulation. For the continuum background, we use the following function [10]:

$$f_{q\bar{q}}(m) = m \sqrt{1 - m^2} e^{-\kappa(1 - m^2)},$$

where $m = m_{ES}/m_{ES}^{\max}$ and m_{ES}^{\max} is the endpoint of the m_{ES} distribution.

For a given B decay mode, the signal m_{ES} distribution is commonly described by a gaussian and a power law [11]. Since the B_{tag} signal consists of many individual decay modes, a single function of that type fails to describe our m_{ES} distribution. We have found that a more general *ansatz* using a gaussian shape $f_g(x) = e^{-x^2/2}$ and a function with a similar shape near $x = 0$, but behaving like e^{-x} for $x \rightarrow \pm\infty$, $f_t(x) = e^{-x}/(1 + e^{-x})^2$, yields a good description of our signal m_{ES} shape:

$$f_{\text{sig}}(\Delta) = \begin{cases} \frac{C_2}{(C_3 - \Delta)^n} & \text{if } \Delta < \alpha \\ \frac{C_1}{\sigma_L} f_t\left(\frac{\Delta}{\sigma_L}\right) & \text{if } \alpha \leq \Delta < 0 \\ \frac{r}{\sigma_1} f_t\left(\frac{\Delta}{\sigma_1}\right) + \frac{1-r}{\sigma_2} f_g\left(\frac{\Delta}{\sigma_2}\right) & \text{if } \Delta \geq 0 \end{cases}, \quad (1)$$

with $\Delta = m_{ES} - \bar{m}_{ES}$ and \bar{m}_{ES} being the maximum of the m_{ES} distribution. C_1 , C_2 and C_3 are functions of the parameters \bar{m}_{ES} , r , σ_1 , σ_2 , σ_L , α and n to ensure that f_{sig} is continuous and differentiable at $\Delta = 0$ and $\Delta = \alpha$. This function, similar to the one featured in [11], describes the tails caused by the asymmetric energy resolution of neutral pions by a power law of order $-n$ and a junction $\alpha < 0$ where it turns into a gaussian-like shape. Fixing α and n to the values obtained from a fit to MC-simulated m_{ES} distributions of signal B_{tag} candidates, we fit a linear combination of $f_{q\bar{q}}$, $f_{b\bar{b}}$ and f_{sig} to the m_{ES} distributions observed in data, leaving all other parameters and normalizations free in the fit (Fig. 1). Due to their similar m_{ES} distributions, this method cannot distinguish between signal B_{tag} candidates and $D^{*-} \leftrightarrow \bar{D}^{*0}$ cross feed. This background contribution is estimated from the MC simulation to be 0.5% (2.6%) relative to the signal for the neutral (charged) B_{tag} sample.

To validate this extraction method, we perform the same analysis on our Monte Carlo sample and find that it reproduces the original number of signal B_{tag} candidates. Uncertainties related to the MC simulation of the combinatoric B_{tag} background are evaluated by decomposing this background into the true underlying individual exclusive decay modes, and varying their contributions by the uncertainties of their branching fractions if they are reported in [9], or $\pm 100\%$ otherwise. This leads to an uncertainty of 1.3% on the number of B^0 and B^+ tags. Due to the different compositions of the combinatoric B^0 and B^+ backgrounds, these errors are uncorrelated. In contrast, systematic errors related to the description of the signal shape are correlated since we use similar decay modes. Here we assess the uncertainties related to the modeling of the shape for $m_{ES} < \bar{m}_{ES}$ by repeating the fit with α set to $-\infty$, allowing an exponential function only instead of a power law to describe the tail caused by the π^0 energy resolution. This leads to relative uncertainties of 2.1% (2.4%) on the number of B^0 (B^+) tags. The yields of events in which B_{tag} candidates have been found for both “twins” of decay channels (II)-(V) differ by 20% in data and MC, motivating a relative uncertainty of 20% on the $D^{*-} \leftrightarrow \bar{D}^{*0}$ cross-feed. This adds another systematic uncertainty of 0.5% to the number of charged B_{tag} candidates. The final numbers of neutral and charged signal B_{tag} candidates are $N_{B^0} = 45420 \pm 420_{(\text{stat})} \pm 591_{(u)} \pm 949_{(c)}$ and $N_{B^+} = 41948 \pm 463_{(\text{stat})} \pm 596_{(u)} \pm 1020_{(c)}$, where u and c denote uncorrelated and correlated systematic uncertainties respectively.

The requirement of an identified electron leads to significantly lower B_{tag} backgrounds, as shown in Fig. 2 for the right-sign sample. For high electron momenta ($p_e > 1 \text{ GeV}/c$), the purities are 96% (98%) for the right-sign (wrong-sign) samples, with combinatoric B_{tag}

candidates being the dominant background, while for decreasing electron momenta, the purities decrease to 90% because of an increasing amount of continuum-background. As for the full B_{tag} sample, we estimate these backgrounds from the m_{ES} sideband region. The background estimates are performed separately for each sample as functions of p_e . Due to low statistics, we do not determine the extrapolation factor from a fit, but use the MC predictions instead. The systematic errors due to the shape of the combinatoric background and $D^{*-} \leftrightarrow \bar{D}^{*0}$ cross feed are evaluated in the same way as for the B_{tag} sample, and the uncertainty in the continuum contribution is taken to be 20%.

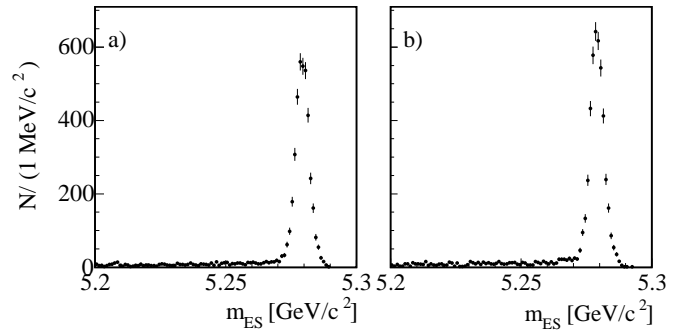


FIG. 2: m_{ES} distributions for (a) neutral and (b) charged B_{tag} candidates in events with a right-sign electron.

Figure 3 shows the momentum spectra of right- and wrong-sign electrons in events with a charged B_{tag} candidate, together with the estimated B_{tag} background. This figure also displays the background contributions of electrons from photon conversions, $\pi^0 \rightarrow \gamma e^+ e^-$ Dalitz decays and misidentified hadrons. These backgrounds are identified and corrected for as in [3, 4]. Corrections for electron identification efficiency and the evaluation of its systematic uncertainty are also performed as in [3, 4].

Background contributions from decays of charmed mesons produced in $b \rightarrow c\bar{s}$ decays or decays of τ leptons are estimated from the MC simulation, using the ISWG2 model [12] to describe semileptonic D and D_s meson decays. Assuming $\Gamma(D_s \rightarrow Xe\nu) = \Gamma(D \rightarrow Xe\nu)$, we obtain $\mathcal{B}(D_s \rightarrow Xe\nu) = (8.05 \pm 0.66)\%$. Inclusive D_s production has been measured in [13] separately for neutral and charged B decays, and with [14] we obtain $\mathcal{B}(B^0 \rightarrow D_s^+ \rightarrow e^+) = (0.67 \pm 0.17)\%$ and $\mathcal{B}(B^+ \rightarrow D_s^+ \rightarrow e^+) = (0.88 \pm 0.18)\%$. Combining the measurements of inclusive D^0 and D^+ production from [13] with the inclusive $D^{0,+} \rightarrow e$ branching fractions from [9] yields $\mathcal{B}(B^0 \rightarrow D^{+,0} \rightarrow e^+) = (0.83 \pm 0.25)\%$ and $\mathcal{B}(B^+ \rightarrow D^{+,0} \rightarrow e^+) = (1.33 \pm 0.20)\%$. Since there are no branching fraction measurements for $B \rightarrow \tau$ decays that distinguish between neutral and charged B decays,

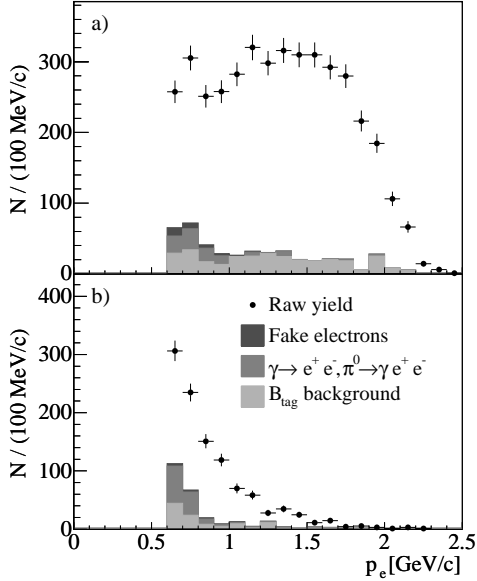


FIG. 3: Total measured spectrum (points) and estimated backgrounds (histograms) for electron candidates in events with a charged B_{tag} candidate, for (a) the right-sign sample, and (b) the wrong-sign sample.

we assume $\Gamma(B^0 \rightarrow X\tau\nu) = \Gamma(B^+ \rightarrow X\tau\nu)$ and combine the average value from [9] with the B -meson lifetimes from direct measurements [9]. Including τ leptons that originate from $B \rightarrow D_s \rightarrow \tau$ cascades, we arrive at $\mathcal{B}(B^0 \rightarrow \tau \rightarrow e^+) = (0.53 \pm 0.06)\%$ and $\mathcal{B}(B^+ \rightarrow \tau \rightarrow e^+) = (0.60 \pm 0.06)\%$. Since the branching fractions of B decays to J/ψ and $\psi(2S)$ mesons are small and well measured, we use the MC simulation to correct for background electrons from $J/\psi \rightarrow e^+ e^-$ and $\psi(2S) \rightarrow e^+ e^-$ decays, using $\mathcal{B}(B \rightarrow J/\psi \rightarrow e^+ e^-) = (6.49 \pm 0.22) \times 10^{-4}$ and $\mathcal{B}(B \rightarrow \psi(2S) \rightarrow e^+ e^-) = (0.23 \pm 0.02) \times 10^{-4}$ [9].

After all corrections listed in Table I have been applied, the inclusive momentum spectrum of electrons from semileptonic decays of B^+ mesons $dN_{B^+ \rightarrow Xe\nu}/dp$ is given by the right-sign sample in B^- -tagged events. Because of $B^0 \bar{B}^0$ oscillations, electrons from $B^0 \rightarrow Xe\nu$ decays and $B^0 \rightarrow \bar{D}X, \bar{D} \rightarrow e^- \nu_e Y$ cascades contribute to both momentum spectra $dN_{\bar{B}^0}^{\text{rs}}/dp$ and $dN_{\bar{B}^0}^{\text{ws}}/dp$ of right- and wrong-sign samples in \bar{B}^0 -tagged events,

$$\frac{dN_{\bar{B}^0}^{\text{rs}}}{dp} = \frac{dN_{B^0 \rightarrow Xe\nu}}{dp}(1 - \chi_m) + \frac{dN_{B^0 \rightarrow \bar{D} \rightarrow Xe\nu}}{dp}\chi_m ,$$

$$\frac{dN_{\bar{B}^0}^{\text{ws}}}{dp} = \frac{dN_{B^0 \rightarrow Xe\nu}}{dp}\chi_m + \frac{dN_{B^0 \rightarrow \bar{D} \rightarrow Xe\nu}}{dp}(1 - \chi_m) ,$$

with $\chi_m = (0.186 \pm 0.004)$ [9] being the $B^0 \bar{B}^0$ mixing parameter. We use these equations to determine the primary electron spectrum $dN_{B^0 \rightarrow Xe\nu}/dp$ of neutral B decays, which is shown in Fig. 4 together with

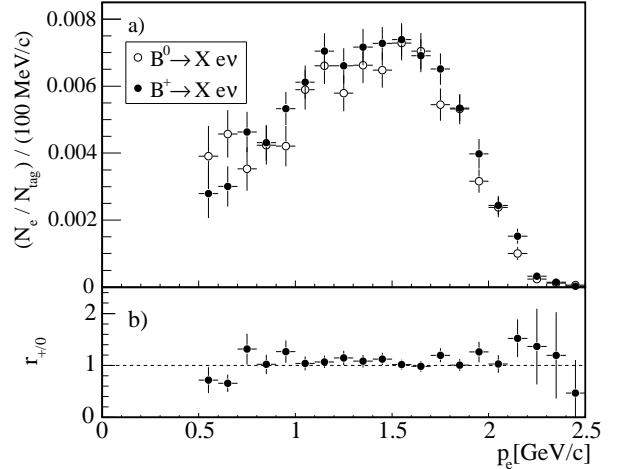


FIG. 4: (a) Normalized momentum spectra of primary electrons after all efficiency corrections and (b) their ratio $r_{+0} = N_{B^0}/N_{B^+}$ ($dN_{B^+ \rightarrow Xe\nu}/dp$) / ($dN_{B^0 \rightarrow Xe\nu}/dp$).

$dN_{B^+ \rightarrow Xe\nu}/dp$ after normalizations to the respective number of tags.

We integrate these spectra between $p_{\min} = 0.6 \text{ GeV}/c$ and $2.5 \text{ GeV}/c$ and apply corrections for geometrical acceptance ($\epsilon_{\text{geom}} = 85\%$) and the small loss of electrons due to bremsstrahlung in the detector material ($\epsilon_{\text{brem}} = 97.4 \pm 0.1\%$) to obtain the partial branching fractions $\hat{\mathcal{B}}(B^0 \rightarrow Xe\nu(\gamma)) = \mathcal{B}(B^0 \rightarrow Xe\nu(\gamma), p_e > p_{\min})$ for decays with any number of photons in the final state:

$$\hat{\mathcal{B}}(B^0 \rightarrow Xe\nu(\gamma)) = (9.66 \pm 0.27_{\text{stat}} \pm 0.32_{\text{syst}})\% ,$$

$$\hat{\mathcal{B}}(B^+ \rightarrow Xe\nu(\gamma)) = (10.39 \pm 0.26_{\text{stat}} \pm 0.37_{\text{syst}})\% ,$$

$$\hat{\mathcal{B}}(B \rightarrow Xe\nu(\gamma)) = (10.03 \pm 0.19_{\text{stat}} \pm 0.32_{\text{syst}})\% .$$

Table II lists the contributions to the systematic errors. These results are in agreement with [1, 3, 4]. For the ratio of branching fractions, $R_{+0}(p_{\min}) = \mathcal{B}(B^+ \rightarrow Xe\nu(\gamma), p_e > p_{\min})/\mathcal{B}(B^0 \rightarrow Xe\nu(\gamma), p_e > p_{\min})$, the result is $R_{+0}(0.6 \text{ GeV}/c) = 1.076 \pm 0.040_{\text{stat}} \pm 0.029_{\text{syst}}$. For higher values of p_{\min} , the statistical error increases, while the systematic error decreases. At $p_{\min} = 1 \text{ GeV}/c$, the combined statistical and systematic error is minimal, leading to our final result

$$R_{+0}(1.0 \text{ GeV}/c) = 1.084 \pm 0.041_{\text{stat}} \pm 0.025_{\text{syst}} .$$

In summary, we have used electrons in $\Upsilon(4S)$ decays tagged by a fully reconstructed hadronic B decay to measure the inclusive semileptonic branching fractions of B^0 and B^+ mesons. The ratio of branching fractions, $R_{+0}(1.0 \text{ GeV}/c) = 1.084 \pm 0.048$, is consistent with the ratio of B lifetimes from direct measurements, $\tau_{B^+}/\tau_{B^0} = 1.086 \pm 0.017$ [9]. From this we conclude that

TABLE I: Electron yields for the four samples and corrections with statistical and systematic errors.

	B^0 tags, right-sign	B^0 tags, wrong-sign	B^+ tags, right-sign	B^+ tags, wrong-sign
$5.27 < m_{ES}(B_{tag}) < 5.29 \text{ GeV}/c^2$	3461 ± 59	1943 ± 44	4074 ± 64	1070 ± 33
B_{tag} background	$198 \pm 16 \pm 40$	$135 \pm 13 \pm 27$	$320 \pm 24 \pm 64$	$114 \pm 12 \pm 23$
$\gamma \rightarrow e^+e^-$	$55 \pm 14 \pm 8$	$87 \pm 17 \pm 12$	$66 \pm 14 \pm 10$	$83 \pm 16 \pm 11$
$\pi^0 \rightarrow \gamma e^+e^-$	$31 \pm 14 \pm 7$	$25 \pm 12 \pm 5$	$36 \pm 14 \pm 7$	$47 \pm 16 \pm 9$
fake e	$29 \pm 1 \pm 8$	$21 \pm 1 \pm 4$	$37 \pm 1 \pm 12$	$16 \pm 0 \pm 2$
Yield before and after e efficiency correction	$3149 \pm 64 \pm 42$	$1674 \pm 51 \pm 30$	$3616 \pm 71 \pm 66$	$810 \pm 41 \pm 27$
	$3443 \pm 70 \pm 71$	$1842 \pm 56 \pm 50$	$3947 \pm 78 \pm 96$	$898 \pm 46 \pm 41$
$B \rightarrow (D_s \rightarrow) \tau \rightarrow e$	$92 \pm 9 \pm 8$	$20 \pm 4 \pm 2$	$109 \pm 10 \pm 9$	0
$B \rightarrow D_s \rightarrow e$	$65 \pm 9 \pm 16$	$13 \pm 4 \pm 3$	$96 \pm 11 \pm 20$	0
$B \rightarrow D \rightarrow e$	$61 \pm 8 \pm 25$	$12 \pm 4 \pm 5$	$96 \pm 11 \pm 15$	0
$B \rightarrow J/\psi, \psi(2S) \rightarrow e$	$22 \pm 5 \pm 1$	$23 \pm 5 \pm 1$	$17 \pm 4 \pm 1$	$18 \pm 4 \pm 1$
$D^{*-} \leftrightarrow \bar{D}^{*0}$ cross feed	$9 \pm 3 \pm 5$	$4 \pm 2 \pm 2$	$44 \pm 7 \pm 22$	$29 \pm 5 \pm 15$
Net e yield	$3195 \pm 72 \pm 82$	$1769 \pm 57 \pm 51$	$3585 \pm 81 \pm 106$	$850 \pm 47 \pm 45$

TABLE II: Breakdown of systematic errors on partial branching fractions $\hat{\mathcal{B}}$ and the ratio $R_{+/0}$. Contributions in the upper part of this table are taken to be uncorrelated for B^0 and B^+ .

	$\Delta \hat{\mathcal{B}}^0[10^{-2}]$	$\Delta \hat{\mathcal{B}}^+[10^{-2}]$	$\Delta R_{+/0}[10^{-2}]$	
$p_{min}[\text{GeV}/c]$	0.6	0.6	0.6	1.0
$N_{tags}(\text{uncorr.})$	0.126	0.141	0.020	0.020
B_{tag} background	0.079	0.122	0.014	0.012
$B \rightarrow D$	0.079	0.041	0.011	0.001
$B \rightarrow D_s$	0.050	0.054	0.008	0.002
χ	0.037		0.004	0.006
$D^{*-} \leftrightarrow \bar{D}^{*0}$	0.014	0.064	0.004	0.003
$B \rightarrow \tau$	0.019	0.020	0.003	0.002
$N_{tags}(\text{corr.})$	0.202	0.253	0.004	0.004
e eff	0.134	0.143	<0.001	
track eff.	0.085	0.092	<0.001	
$D, D_s, \tau \rightarrow e$	0.024	0.020	<0.001	
conversion, Dalitz	0.025	0.039	0.001	<0.001
faked e	0.020	0.027	<0.001	

the semileptonic decay widths of charged and neutral B mesons agree to a precision of 5%, $\Gamma(B^0 \rightarrow Xe\nu) / \Gamma(B^+ \rightarrow Xe\nu) = 0.998 \pm 0.047$.

We are grateful for the excellent luminosity and machine conditions provided by our PEP-II colleagues, and for the substantial dedicated effort from the computing organizations that support *BABAR*. The collaborating institutions wish to thank SLAC for its support and kind hospitality. This work is supported by DOE and NSF (USA), NSERC (Canada), IHEP (China), CEA and CNRS-IN2P3 (France), BMBF and DFG (Germany),

INFN (Italy), FOM (The Netherlands), NFR (Norway), MIST (Russia), and PPARC (United Kingdom). Individuals have received support from the A. P. Sloan Foundation, Research Corporation, and Alexander von Humboldt Foundation.

- * Also with Università di Perugia, Dipartimento di Fisica, Perugia, Italy
- † Also with Università della Basilicata, Potenza, Italy
- [1] T. Okabe *et al.* (*Belle* Collaboration), Phys. Lett. B **614** (2005) 27.
- [2] M. Artuso *et al.* (*CLEO* Collaboration), Phys. Lett. B **399** (1997) 321.
- [3] B. Aubert *et al.* (*BABAR* Collaboration), Phys. Rev. D **69** (2004) 111104.
- [4] B. Aubert *et al.* (*BABAR* Collaboration), Phys. Rev. D **67** (2003) 031101.
- [5] B. Aubert *et al.* (*BABAR* Collaboration), Nucl. Instr. Meth. **A479**, 1 (2003).
- [6] S. Agostinelli *et al.* (*GEANT4* Collaboration), Nucl. Instr. Meth. **A506**, 250 (2003).
- [7] G.C. Fox and S. Wolfram, Phys. Rev. Lett. **41**, 1581 (1978).
- [8] Charge conjugation is implied throughout the paper.
- [9] S. Eidelman *et al.*, Phys. Lett. B **592**, 1 (2004).
- [10] H. Albrecht *et al.* (*ARGUS* Collaboration), Z. Phys. C **48**, 543 (1990).
- [11] $CB(m_{ES}) = e^{-\alpha^2/2}(n/|\alpha|)^n(n/|\alpha| - |\alpha| - y)$ for $y < \alpha$, $CB(m_{ES}) = e^{-y^2/2}$ for $y > \alpha$, where $y \equiv (m_{ES} - \bar{m}_{ES})/\sigma$. D. Antreasyan, Crystal Ball Note 321 (1983).
- [12] D. Scora and N. Isgur, Phys. Rev. D **52**, 2783 (1995).
- [13] B. Aubert *et al.* (*BABAR* Collaboration), Phys. Rev. D **70**, 091106 (2004).
- [14] B. Aubert *et al.*, (*BABAR* Collaboration), Phys. Rev. D

71, 091104 (2005).